

## A KECK DEIMOS KINEMATIC STUDY OF ANDROMEDA IX: DARK MATTER ON THE SMALLEST GALACTIC SCALES

SCOTT C. CHAPMAN,<sup>1</sup> RODRIGO IBATA,<sup>2</sup> GERAINT F. LEWIS,<sup>3</sup> ANNETTE M. N. FERGUSON,<sup>4</sup>

MIKE IRWIN,<sup>5</sup> ALAN MCCONNACHIE,<sup>5</sup> AND NIAL TANVIR<sup>6</sup>

Received 2005 February 2; accepted 2005 September 6; published 2005 October 3

### ABSTRACT

We present the results of a kinematic survey of the dwarf spheroidal satellite of M31, And IX, which appears to be the lowest surface brightness and also the faintest galaxy ( $M_V = -8.3$ ) found to date. Using Keck DEIMOS spectroscopic data, we have measured its velocity relative to M31, its velocity dispersion, and its metallicity. It exhibits a significant velocity dispersion  $\sigma_v = 6.8^{+3.0}_{-2.0}$  km s<sup>-1</sup>, which coupled with the low luminosity implies a very high mass-to-*V*-band light ratio,  $M/L \sim 93^{+120}_{-50} M_\odot/L_\odot$  ( $M/L > 17 M_\odot/L_\odot$  at 99% confidence). Unless strong tidal forces have perturbed this system, this smallest of galaxies is a highly dark matter-dominated system.

*Subject headings:* galaxies: dwarf — galaxies: evolution —  
galaxies: individual (Andromeda V, Andromeda IX) — Local Group

### 1. INTRODUCTION

Hierarchical structure formation models, such as  $\Lambda$ CDM, predict that large spiral galaxies like the Milky Way or Andromeda (M31) arise from successive mergers of small galaxies and from the smooth accretion of gas. At late times, when a dominant central mass is in place, the main mode of mass acquisition is via the cannibalization of low-mass satellites that fall into the gravitational potential well of the massive host. These  $\Lambda$ CDM models are highly successful at explaining observations on large scales. However, the models predict an overabundance of low-mass dark subhalos, which is inconsistent by 1–2 orders of magnitude with the number of observed dwarf galaxies (Klypin et al. 1999; Moore et al. 1999; Benson et al. 2002b). Large uncertainties remain on the level of disagreement between model and observation because of the difficulty in constraining the faint end of the galaxy luminosity function; the low surface brightnesses expected for the faintest galaxies ( $\mu_V \geq 26$  mag arcsec<sup>-2</sup>; e.g., Caldwell 1999; Benson et al. 2002a) imply that ground-based surveys are likely incomplete even in nearby galaxy groups. From a theoretical perspective, star formation in low-mass subsystems would have to be suppressed (e.g., photoionization in the early universe) to bring models and observations into closer accord. The result of this hydrodynamical modification would be a shallower faint-end slope for the  $z \sim 0$  galaxy luminosity function (e.g., Somerville 2002; Benson et al. 2002a; Willman et al. 2004). A critical prediction of this solution is that dwarf galaxies should then be embedded in much larger, more massive dark subhalos (Stoehr et al. 2002).

Observational progress can be made in the case of the Local Group (LG), where galaxies can be resolved into stars, thereby probing much fainter effective surface brightness limits (Ibata

et al. 2001; Ferguson et al. 2002; Lewis et al. 2004; Willman et al. 2005). Of particular interest is the system And IX, which was first reported by the Sloan Digital Sky Survey team (Zucker et al. 2004) and is visible in previously published maps from the M31 Isaac Newton Telescope (INT) Wide-Field Camera (WFC) survey (Ferguson et al. 2002). And IX is one of the lowest surface brightness galaxies found to date ( $\mu_{V,0} \sim 26.8$  mag arcsec<sup>-2</sup>), and at the distance estimated from the position of the tip of the red giant branch [RGB;  $I = 20.50 \pm 0.03$ ,  $M_I^{\text{TRGB}} = 4.065$ ,  $(m - M)_0 \sim 24.42$ ] of  $765 \pm 24$  pc (McConnachie et al. 2005), And IX would also be one of the faintest galaxies known ( $M_V = -8.3$ ). It therefore has the potential to place strong constraints on both the LG luminosity function and the physics of galaxy formation at the smallest scales. In this Letter, we present the results of a kinematic survey of the And IX dwarf spheroidal (dSph) satellite of M31. We have assumed for this Letter a distance to M31 of  $785 \pm 25$  kpc [ $(m - M)_0 = 24.47 \pm 0.07$ ; McConnachie et al. 2005].

### 2. PROPERTIES OF AND IX

And IX reveals itself in the INT WFC survey data as an enhancement of metal-poor RGB stars at a location of 1:8 to the east and 1:9 to the north of the nucleus of M31. Figure 1 shows a color-magnitude diagram (CMD) centered on And IX and a nearby comparison region of equivalent area. The excess RGB stars on the blueward side of the general M31 RGB locus form a well-defined And IX locus with an apparent RGB tip at  $I = 20.5$  consistent with the distance of M31, and if representative of an old stellar population,  $[\text{Fe}/\text{H}] \sim -1.5$  (McConnachie et al. 2005). Although sparsely populated, the radial profile, computed as the median counts in circular annuli centered on  $00^{\text{h}}52^{\text{m}}52^{\text{s}}$ ,  $+43^{\circ}12'00''$ , is well defined and is shown background-corrected in the right-hand panel of Figure 2. Exponential and Plummer law profiles provide adequate fits, with the scale radius from the exponential fit being  $r_e = 1:4 \pm 0:3$  (corresponding to  $r_s = 315 \pm 65$  pc; half-light radius  $r_h = 530 \pm 110$  pc—including background subtraction errors), a value comparable to the other Andromedan dSph companions (Mateo 1998; Caldwell 1999; McConnachie & Irwin 2005).

The luminosity of the dwarf galaxy is constrained by measuring the integrated flux, or surface brightness, distribution. The processing procedure (Irwin et al. 2004) takes existing derived object catalogs to define a “bright” foreground star

<sup>1</sup> California Institute of Technology, 1200 East California Boulevard, Pasadena, CA 91125; schapman@astro.caltech.edu.

<sup>2</sup> Observatoire de Strasbourg, 11 rue de l’Université, F-67000 Strasbourg, France.

<sup>3</sup> Institute of Astronomy, School of Physics, A29, University of Sydney, NSW 2006, Australia.

<sup>4</sup> Institute for Astronomy, University of Edinburgh, Royal Observatory, Blackford Hill, Edinburgh EH9 3HJ, UK.

<sup>5</sup> Institute of Astronomy, University of Cambridge, Madingley Road, Cambridge CB3 0HA, UK.

<sup>6</sup> Centre for Astrophysics Research, University of Hertfordshire, Hatfield AL10 9AB, UK.

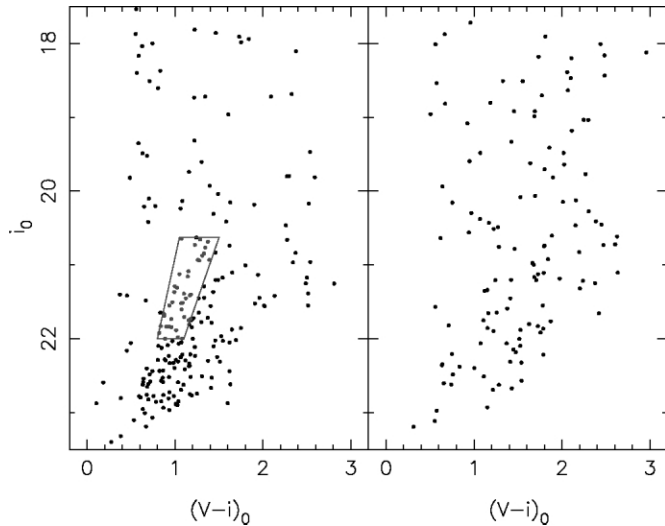


FIG. 1.—*Left panel*: Color-magnitude diagram from a region centered on And IX with radius  $2.5'$ . The quadrilateral shows the adopted CMD selection box, designed to select And IX RGB stars, which are blue and metal-poor, for spectroscopic follow-up. *Right panel*: a comparison region of the same size  $10'$  to the north.

component, 1 mag above the RGB tip (to allow for potential asymptotic giant branch stars); a circular aperture is excised around each foreground star and the flux within set to the local sky level interpolated from a whole-frame background map (the size of the aperture is the maximum of 4 times the catalog-recorded area at the detection isophote or a diameter 4 times the derived FWHM seeing); each frame is then rebinned on a  $3 \times 3$  grid to effectively create  $1''$  pixels; the binned image is then further smoothed using a two-dimensional Gaussian filter of FWHM  $5''$ , producing a coarsely sampled smooth image containing both the resolved and unresolved light contribution from the dwarf. The background is determined by robustly fitting a smoothly varying surface over the whole mosaic area. The central surface brightness is measured by deriving the radial profile, defined as the background-corrected median flux value within elliptical annuli. The variation in the flux from the multiple background measures gives a good indication of the flux error (dominated by systematic fluctuations). Since the systematics are dominated by random residual foreground star halos and scattered light from bright stars, possibly just outside the field of view, we mitigate the effect by defining the size of the elliptical aperture to be equivalent to the geometric half-light radius derived from the number density profile. The estimated total flux is then scaled to allow for this correction. In this way, we derive  $M_V = -8.3 \pm 0.2$  (corrected for extinction), in agreement with the estimate of  $M_V = -8.3$  from Zucker et al. (2004), and measure a central surface brightness  $\Sigma_V = 26.5 \pm 0.3$  mag arcsec $^{-2}$ .

### 3. SPECTROSCOPIC OBSERVATIONS AND DATA ANALYSIS

Spectra for And IX were obtained with the DEep Imaging Multi-Object Spectrograph (DEIMOS) on the Keck II telescope on the night of 2004 September 13, under photometric conditions and seeing from  $0.5''$  to  $0.8''$ . We employed the 1200 line mm $^{-1}$  grating covering the wavelength range 6400–9000 Å, with a spectral resolution of  $\sim 1.5$  Å. The observations pioneered a new approach with DEIMOS using a “fiber hole”  $0.7''$  slitlet (to match the median seeing) approach with 623 holes assigned within the  $16' \times 5'$  DEIMOS mask, giving Poisson-limited sky subtraction

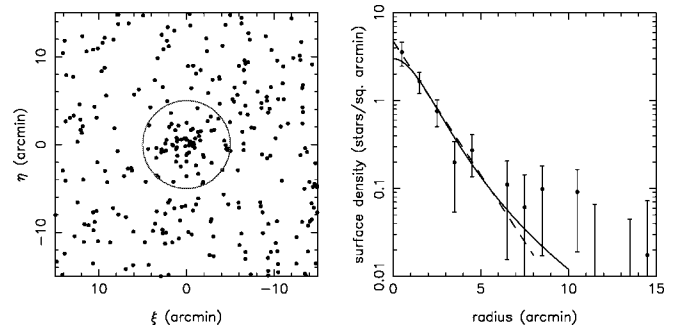


FIG. 2.—*Left panel*: Positions of the stars in a  $15' \times 15'$  region around the center of And IX that fall in the RGB selection box of Fig. 1. The  $5'$  radius circle used for selecting radial velocity members is also displayed. *Right panel*: Surface density profile of these RGB stars with a background component removed. This background was modeled with a sloping component that is a function of the radial distance to the center of M31; at the position of And IX, the background has a number density of  $0.26 \pm 0.08$  arcmin $^{-2}$ . The overlaid profiles are a Plummer model (*solid line*) with central density  $3.0$  arcmin $^{-2}$  and scale size  $2.6'$  and an exponential profile (*dashed line*) with central density  $4.8$  arcmin $^{-2}$  and scale size  $1.4'$ .

(down to  $i = 21.5$ ) by assigning holes to monitor the sky spectrum. Stars were selected for observation primarily within a color-magnitude box designed to choose RGB stars from the  $5'$  region surrounding And IX. This color-magnitude selection box is displayed in Figure 1. We then let the DEIMOS configuration program randomly choose objects as fillers with  $I$ -band magnitudes  $20.5 < I < 22.0$  and colors  $1.0 < V - i < 4.0$ . Both metal-poor and metal-rich populations will be present in this selection. A total of 289 stars and 334 sky slits were assigned in this low-density field in the M31 outer halo.

The And IX mask was observed for three integrations of 20 minutes each. The spectroscopic images were processed and combined using the pipeline software developed by our group (debiases, performs a flat field, extracts, wavelength-calibrates, and sky-subtracts the spectra). The radial velocities of the stars were then measured with respect to a Gaussian model of the Ca II triplet lines (similar to the technique of Wilkinson et al. 2004). By fitting the three Ca triplet lines separately, an estimate of the radial velocity accuracy was obtained for each radial velocity measurement. The measurements have typical uncertainties of 5–10 km s $^{-1}$ . A sample of 138 stars yielded a continuum signal-to-noise ratio (S/N)  $> 10$  and cross-correlations with velocity uncertainties of less than 15 km s $^{-1}$ , and we include only these stars in the subsequent analysis; 18 of these 138 stars lie in the And IX color selection window.

The measured radial velocities in the And IX field are shown in Figure 3 as a function of radial distance from the galaxy. A strong foreground Galactic component is present at heliocentric velocities  $v > -150$  km s $^{-1}$ , though as we show in a companion paper (Ibata et al. 2005), below this velocity the Galactic contamination is small. Close to the center of And IX there is a small but clear kinematic grouping of stars that also lie on the And IX RGB. We first define an inner sample to be the five stars observed within a radius of one exponential scale length ( $1.4'$ ); this sample has a mean of  $v = -210.1$  km s $^{-1}$  and an rms dispersion of  $\sigma_v = 5.2$  km s $^{-1}$ , which is tiny compared to the huge velocity spread of stars beyond  $5'$ , indicating that the sample is highly unlikely to be contaminated. Indeed, outside of a radius of  $5'$  not a single RGB-selected star is found within 80 km s $^{-1}$  of this mean.

Figure 3 shows that all stars within the RGB selection box in a radius of  $5'$  have radial velocities close to the mean of the inner sample. A fit of a maximum likelihood Gaussian model

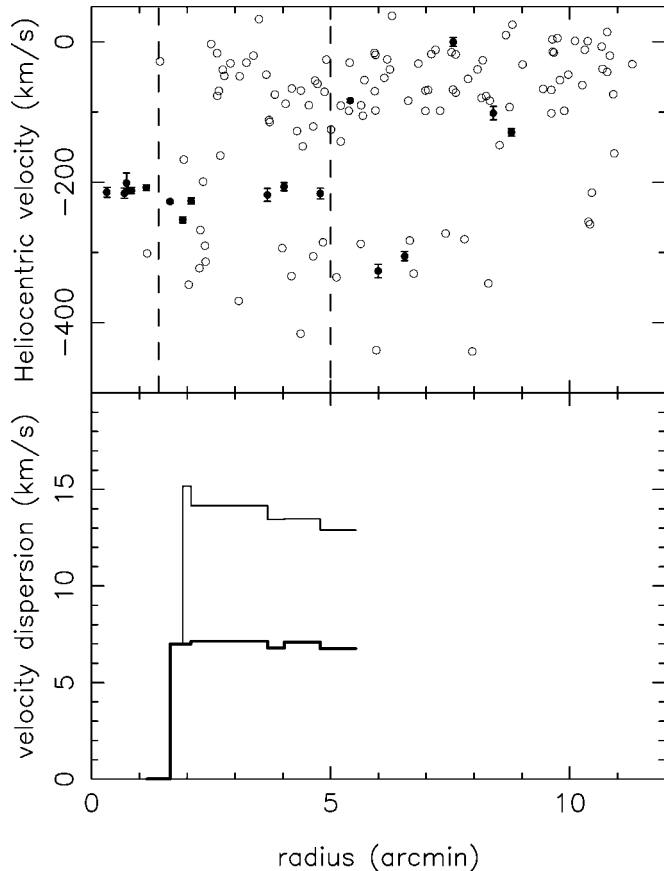


FIG. 3.—*Upper panel*: Radial velocities of all stars with velocity uncertainty  $< 15 \text{ km s}^{-1}$  from the fiber hole mask centered on And IX. Filled circles mark the data for the stars in the color-magnitude selection box of Fig. 2; open circles are other targets. The dashed lines indicate the radial selection limits discussed in the text. *Lower panel*: Derived maximum likelihood velocity dispersion as a function of radius; the thin line corresponds to all the data, while the thick line rejects one velocity outlier situated at  $1.9'$ .

given these data (and their uncertainties) is shown on the left-hand panel of Figure 4 (*thin black lines*), where we display the likelihood contours as a function of mean velocity and velocity dispersion. The most likely values are  $v = -219 \pm 4 \text{ km s}^{-1}$  and  $\sigma_v = 12.9^{+4}_{-2} \text{ km s}^{-1}$ . However, a single star at  $1.9'$  stands out in this sample of 11 objects as it is offset by  $-44.6 \text{ km s}^{-1}$  from the mean velocity of the inner sample. Since this object is potentially a contaminant, it is important to make an estimate of the expected contribution from M31 in the larger  $5'$  sample. We find that the halo in our kinematic survey of M31, as seen through windows not affected by the M31 disk or by Galactic stars (S. C. Chapman, R. Ibata, A. M. N. Ferguson, M. Irwin, G. Lewis, & N. Tanvir 2005, in preparation), can be approximated to first order with a Gaussian distribution of dispersion  $99 \text{ km s}^{-1}$ , centered at a mean velocity of  $-300 \text{ km s}^{-1}$ . We use the RGB-selected stars at radii larger than  $5'$  and with velocities  $v < -300 \text{ km s}^{-1}$  (there are two such stars) to normalize this simple halo model in the present field. A crude estimate of the expected contamination within a velocity interval of  $\pm 44.6 \text{ km s}^{-1}$  of the mean velocity of the inner sample can then be made ( $\approx 0.2$  stars contaminate the sample within  $5'$ ).

There is therefore some grounds to reject the velocity outlier at  $1.9'$ , resulting in a fit with mean velocity and dispersion of  $v = -216 \pm 3 \text{ km s}^{-1}$  and  $\sigma_v = 6.8^{+3.0}_{-2.0} \text{ km s}^{-1}$ . The lower panel of Figure 3 shows the maximum likelihood velocity dispersion measures, starting at the radius of the inner  $1.4'$  sample and

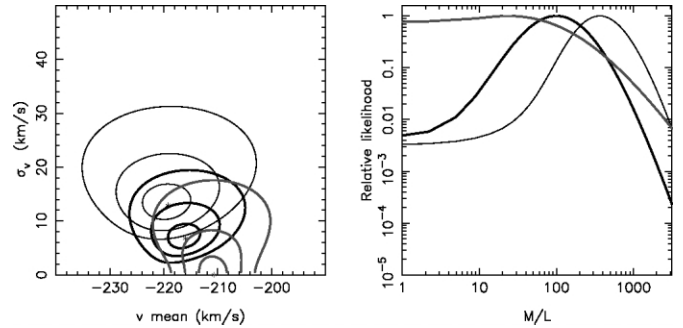


FIG. 4.—*Left panel*: Likelihood contours (at  $1 \sigma$ ,  $2 \sigma$ ,  $3 \sigma$ ) of the mean and dispersion of the And IX population, based on radial velocity data within  $5.0'$  (*black curves*) and  $1.4'$  (*gray curves*). The thick black curves show the effect of rejecting a single datum at  $r = 1.9'$ . The corresponding relative likelihood of different mass-to-light ratios are displayed on the right-hand panel. The thin black line is determined from the sample of 11 stars with  $r < 5'$ , while for the thick black line a single star has been rejected. The gray line shows the result for the  $r < 1.4'$  sample.

moving outward to  $5'$  adding one datum at a time (the thick-lined distribution rejects the velocity outlier at  $1.9'$ ). Evidently, the first five velocity data are consistent with being drawn from a population with zero intrinsic velocity dispersion, though beyond  $1.6'$  the dispersion appears to increase to  $\sim 7 \text{ km s}^{-1}$ . We note in passing that the present data set shows no clear radial velocity gradient. The (maximum likelihood fitted) mean velocity of the five inner stars within  $1.4'$  is  $-210.6 \pm 3 \text{ km s}^{-1}$ , while the mean velocity of the sample of five stars between  $1.4'$  and  $5'$  (with the outlier rejected) is  $-220.4 \pm 4 \text{ km s}^{-1}$ , so the velocity difference between the two samples is less than  $2 \sigma$ .

The spectra also allow a measurement of the metallicity of the dwarf galaxy using the CaT equivalent width (EW) technique. While the S/N of individual stars are typically too low to yield useful estimates of the CaT EWs, we proceeded to measure the average metallicity by stacking the RGB star spectra of the five highest S/N stars of our sample of 10 stars within  $r < 5'$ . We follow as closely as possible the method of Rutledge et al. (1997), fitting Moffat functions to the average Ca II lines and yielding a CaT EW used to estimate the metallicity as  $[\text{Fe}/\text{H}] = -2.66 + 0.42[\Sigma\text{Ca} - 0.64(V_{\text{HB}} - V_{\text{ave}})]$ , with  $\Sigma\text{Ca} = 0.5\text{EW}_{\lambda 8498} + 1.0\text{EW}_{\lambda 8542} + 0.6\text{EW}_{\lambda 8662}$ ,  $V_{\text{HB}}$  being a surface gravity correction relative to the  $V$  magnitude of the horizontal branch and  $V_{\text{ave}} = 22.4 \pm 0.3$  the average magnitude of the And IX stars. We correct the value of  $V_{\text{HB}} = 25.17$  for M31, measured by Holland et al. (1996), by  $-0.06$  mag to account for the difference in line-of-sight distance between M31 and And IX. We find  $[\text{Fe}/\text{H}] = -1.5$  (on the Carretta & Gratton 1997 scale), with a large uncertainty of  $\sim 0.3$  mag, which is due primarily to sky subtraction residuals making it difficult to define the continuum level of the spectrum. This metallicity estimate confirms the previous photometric estimates of  $[\text{Fe}/\text{H}] \sim -1.5$  by McConnachie et al. (2005) and of  $[\text{Fe}/\text{H}] \sim -2$  by Harbeck et al. (2005). A metallicity of  $[\text{Fe}/\text{H}] \sim -2$  would be closer to what we would expect for such a faint dSph; however, if the mass were as large as suggested by the upper range of our kinematic analysis, a metallicity of  $[\text{Fe}/\text{H}] \sim -1.5$  would be reasonable.

#### 4. A COLD DARK MATTER-DOMINATED ACCRETED COMPANION TO M31?

The mean radial velocity that we measure ( $v = -216 \pm 3 \text{ km s}^{-1}$ ) implies that And IX is almost certainly a bound satellite

to M31. The relative radial velocity from M31 is then only ( $\Delta v = 84 \pm 3 \text{ km s}^{-1}$ ), while its separation from the M31 center is only  $\sim 50$  kpc. In the model of Ibata et al. (2004), the escape velocity from 50 kpc is  $550 \text{ km s}^{-1}$ ; if the velocity vector of And IX is uncorrelated with the direction vector to the observer, the chances of measuring a line-of-sight component of only  $84 \text{ km s}^{-1}$  if And IX is unbound would be  $< 1\%$  (although uncertainty in the line-of-sight distance could slightly increase the probability). And IX is therefore most likely bound to M31. The measured velocity dispersion also allows us to constrain the dark matter content of the small galaxy, assuming virial equilibrium. The mass-to-light ratio of a simple spherically symmetric stellar system of central surface brightness  $\Sigma_0$ , half-brightness radius  $r_{\text{hb}}$ , and central velocity dispersion  $\sigma_0$  can be estimated as

$$M/L = \eta \frac{9}{2\pi G \Sigma_0 r_{\text{hb}}} \frac{\sigma^2}{L_\odot} \quad (1)$$

(Richstone & Tremaine 1986), where  $\eta$  is a dimensionless parameter that has a value close to unity for many structural models.

For our sample of stars within  $5'$ , the measured velocity dispersion is not necessarily representative of the central value of  $\sigma_0$ . However, for most models of bound stellar systems like those assumed in the core-fitting method, the velocity dispersion decreases with distance, so that our measured dispersion will be an underestimate of  $\sigma_0$  if And IX conforms to these models. Assuming that  $\sigma_v = \sigma_0$ , we show the relative likelihood of  $M/L$  values for our sample selections on the right-hand panel of Figure 4, where we have folded in the uncertainties in the half-light radius, the velocity dispersion, and the central surface brightness. For the  $5'$  sample with the rejected velocity outlier, we find that the measured kinematics imply that And IX has a mass-to-light ratio  $M/L = 93^{+120}_{-50} M_\odot/L_\odot$  (*thick black line*). In particular, with this sample we can reject the possibility that And IX has  $M/L < 17 M_\odot/L_\odot$  with 99% confidence. However, this measurement depends very sensitively on our adopted sam-

ple; if we do not reject the single most discrepant velocity datum, we find a higher preferred  $M/L$  value (*thin black line*), while if we choose the inner five stars alone (*gray lines*), the mass can be consistent with zero.

The spectroscopic data we have presented here have allowed us to make a preliminary assessment of the mass and nature of this intriguing dwarf galaxy. Our preferred mass estimate ( $\sim 1.6 \times 10^7 M_\odot$ ) implies a substantial dark matter component with a mass-to-light ratio  $\sim 93$  in this faint galaxy. For comparison, applying the same procedure above to the case of the Draco dSph, the most dark matter-dominated of the Milky Way satellites, which has  $\sigma_0 = 8.5 \text{ km s}^{-1}$  (Kleyna et al. 2002),  $r_{\text{hb}} = 120 \text{ pc}$ , and  $\Sigma_0 = 2.2 M_\odot \text{ pc}^{-2}$  (Irwin & Hatzidimitriou 1995), gives  $M/L = 91$  (though more detailed dynamical modeling suggests  $M/L = 440 \pm 240 M_\odot/L_\odot$ ; Kleyna et al. 2002). We point out that this analysis assumes a Gaussian distribution, while there are probably too few And IX data points to support this assumption.

Although we cannot rule out the possibility that tidal effects have enhanced the extent and velocity dispersion of this satellite, yielding a misleadingly high mass-to-light ratio estimate, And IX appears to be a highly dark matter-dominated dSph. It therefore presents an intriguing possibility for hierarchical cold dark matter models of structure formation—that many dark matter-dominated dSphs, fainter even than And IX, and lying just below the limits of detectability, may be present in the halos of giant galaxies like M31, bringing models (e.g., Moore et al. 1999; Benson et al. 2002a) into better accord with data. Nevertheless, given the small size of our sample of stars, further accurate kinematic data are needed to confirm the velocity dispersion measurement, while deep photometry will help ascertain the extent to which tidal forces may be perturbing the system.

We thank the referee, Steve Majewski, for his thorough comments on the manuscript. G. F. L. acknowledges support through ARC DP 0343508. A. M. N. F. has been supported by a Marie Curie Fellowship of the European Community (HPMF-CT-2002-01758).

#### REFERENCES

- Benson, A. J., Frenk, C. S., Lacey, C. G., Baugh, C. M., & Cole, S. 2002a, MNRAS, 333, 177
- Benson, A. J., Lacey, C. G., Baugh, C. M., Cole, S., & Frenk, C. S. 2002b, MNRAS, 333, 156
- Caldwell, N. 1999, AJ, 118, 1230
- Carretta, E., & Gratton, R. 1997, A&AS, 121, 95
- Ferguson, A. M. N., Irwin, M. J., Ibata, R. A., Lewis, G. F., & Tanvir, N. R. 2002, AJ, 124, 1452
- Harbeck, D., Gallagher, J., Grebel, E., Kock, A., & Zucker, D. 2005, ApJ, 623, 159
- Holland, S., Fahlman, G. G., & Richer, H. B. 1996, AJ, 112, 1035
- Ibata, R., Chapman, S. C., Ferguson, A. M. N., Lewis, G., Irwin, M., & Tanvir, N. 2005, ApJ, in press (astro-ph/0504164)
- Ibata, R., Chapman, S. C., Irwin, M., Lewis, G., Ferguson, A. M. N., McConnachie, A., & Tanvir, N. 2004, MNRAS, 351, 117
- Ibata, R., Irwin, M., Lewis, G., Ferguson, A. M. N., & Tanvir, N. 2001, Nature, 412, 49
- Irwin, M., & Hatzidimitriou, D. 1995, MNRAS, 277, 1354
- Irwin, M., et al. 2004, Proc. SPIE, 5493, 411
- Kleyna, J., Wilkinson, M., Evans, N., Gilmore, G., & Frayn, C. 2002, MNRAS, 330, 792
- Klypin, A., Kravtsov, A. V., Valenzuela, O., & Prada, F. 1999, ApJ, 522, 82
- Lewis, G., Ibata, R., Chapman, S., Ferguson, A., McConnachie, A., Irwin, M., & Tanvir, N. 2004, Publ. Astron. Soc. Australia, 21, 203
- Mateo, M. 1998, ARA&A, 36, 435
- McConnachie, A., & Irwin, M. 2005, MNRAS, submitted
- McConnachie, A., Irwin, M., Ibata, R., Lewis, G., Ferguson, A., & Tanvir, N. 2005, MNRAS, 356, 979
- Moore, B., Ghigna, S., Governato, F., Lake, G., Quinn, T., Stadel, J., & Tozzi, P. 1999, ApJ, 524, L19
- Richstone, D. O., & Tremaine, S. 1986, AJ, 92, 72
- Rutledge, G., Hesser, J., & Stetson, P. 1997, PASP, 109, 883
- Somerville, R. S. 2002, ApJ, 572, L23
- Stoehr, F., White, S., Tormen, G., & Springel, V. 2002, MNRAS, 335, L84
- Wilkinson, M., Kleyna, J., Evans, N., Gilmore, G., Irwin, M., & Grebel, E. 2004, ApJ, 611, L21
- Willman, B., et al. 2004, MNRAS, 353, 639
- . 2005, ApJ, 626, L85
- Zucker, D. B., et al. 2004, ApJ, 612, L121